VYSOKÉ UČENÍ TECHNICKÉ V BRNĚ

Fakulta elektrotechniky a komunikačních technologií

Ústav radioelektroniky

Ing. Stanislav Goňa

ANALYSIS AND DESIGN
OF PLANAR REFLECTOR ANTENNAS

ANALÝZA A NÁVRH
PLANÁRNÍCH REFLEKTOROVÝCH ANTÉN

SHORT VERSION OF PH.D. THESIS

Obor:	Elektronika, měřicí a sdělovací technika
Školitel:	Prof. Dr. Ing. Zbyněk Raida
Oponenti:	Prof. Ing. Miloš Mazánek, CSc.
	Prof. Ing. Dušan Černohorský, CSc.
Datum obhajoby:	13. 5. 2004

Keywords

Planar reflector antennas, method of moments, Green's functions, frequency selective surfaces, constrained optimization, printed reflectarrays, finite element method (Ansys)

Klíčová slova

Planární reflektorová anténa, momentová metoda, Greenovy funkce, kmitočtově selektivní povrchy, omezená optimalizace, planární odražeče, metoda konečných prvků (Ansys)

Místo uložení práce

Vědecké oddělení FEKT VUT v Brně, Údolní 53, Brno, 602 00

Contents

1   INTRODUCTION

The planar reflector antennas represent an evolution of the classical curved reflector antennas. The evolution was historically aimed to replace the standard parabolic reflector by a flat one, which can be fabricated more easily and at lower cost than the standard curved reflector. The idea of flat reflectors appeared first in 1960's and relied on the printed technology. These early designs mostly relied on empirical experience with little or no numerical modeling of antennas. Two decades later, the advent of the planar reflector antennas came. But the true boom of the planar reflector antennas occurred during 1990's for two reasons. First, the computational power of the ordinary PC's or workstations was high enough to enable analysis and design of the planar reflector antennas at emerging frequency bands (as Ka or W). Second, the progress in numerical modeling allowed investigation of novel and complex structures.

1.1   PLANAR REFLECTOR ANTENNAS

In contrast to the classical reflector antennas incorporating a curved reflector, the main reflector of the planar reflector antenna consists of the flat antenna body having a substrate on it. The substrate is covered by a passive or active circuitry organized as an array of small rectangular cells (typically sized about half a wavelength ($\lambda_0/2$)). The circuitry adjusts the phase of the outgoing field in the plane of the main reflector. Due to a tight analogy with optics, planar reflector antennas are often called quasi-optical antennas. The analogy allows the designer to rely on the idea of rays traveling from a feeder and reflecting from particular reflectors to finally illuminate the main reflector (see Fig. 1.1).
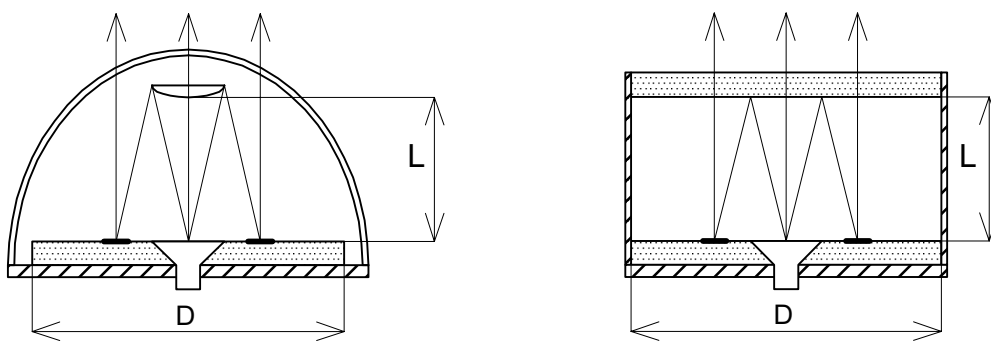

Fig. 1.1   *Simple (left) and folded (right) reflector antenna. Several representative rays are shown to demonstrate the quasi-optical behavior of the antennas.*

Two kinds of planar reflector antennas exist (Fig. 1.1), a simple one [1] and a folded one [2], [3]. The feeding mechanism is the only difference between them. While simple antennas can be either prime focus, Cassegrein, or back-fire illuminated, folded antennas are fed by an auxiliary slot array. The slot array is totally reflecting for one polarization and transparent for the perpendicular one. A change of the plane of polarization occurs after reflection from the main reflector. That reflector thus not only performs phase adjustment but it also does a twisting of the electric field by 90°.

1.1.1 Design of planar reflector antennas

To design planar reflector antenna, an optimization method has to be applied to tune patch dimensions in each cell of the reflectarray: the reflected electric field in each cell is decomposed into components parallel with patch edges (Fig. 1.2), these componets are denoted as E^R_x and $-E^R_y$.
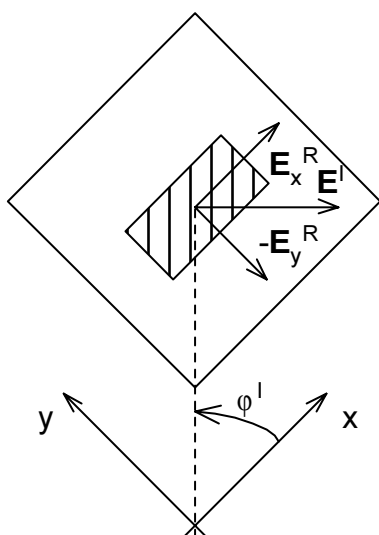

Fig. 1.2

Orientation of the vector of electric field intensity E^I of the incident wave (tangential components) and the components E^R_x, $-E^R_y$ of the reflected wave. Plane of incidence is depicted by a short-dashed line and is described by standard spherical angles ϑ^I (not shown in the figure) and φ^I. Boundary of an elementary cell sized a and b is marked by a long-dashed line.

The phase of componets E^R_x and $-E^R_y$ is expressed as a function of the width and the length of the patch. As the next step, the initial patch dimensions are chosen and an optimization method is applied. The method seeks for patch dimensions which deliver the desired phase of components E^R_x and $-E^R_y$. The present literuture resources give no details about the step. The dissertation uses a kind of the quasi-Newton method to solve the optimization problem (more specifically, Levenberg-Marquardt method is applied).

1.1.2   Analysis of planar reflector antennas

To analyze radiation properties of the designed planar reflector antenna, a superposition approach is used. That approach is represented by a direct summation of fields produced by individual cells [1].

Complete electromagnetic analysis of the designed antenna is problematic. Even if the up-to-date fast mulipole methods are applied. However, analysis of a folded reflector antenna with rectangular patch elements can be performed even without of the fast mulipole: the antenna is analyzed with the help of the spectral domain method of moments (MoM) in conjuction with large domain current basis functions [12]. Since the number of unknows is still relatively high, an extremely numerically efficient evaluation of the double infinite integrals arising in the spectral domain has to be employed. However, an extra care has to be paid to the oscillatory nature of the integrand for electrically distanced patches.

Analysis of reflector antennas by commercial electromagnetic (EM) codes is limited to antennas, whose electric size is not too large. A very few results about EM analysis of planar reflector antennas can be found in the present literature or in conference papers. E.g. in [13], FDTD[1] (code Lc from Cray Reasearch) was employed for the analysis of a double layer printed reflectarray.

Electrically large problems can be also solved by the finite integration technique (FIT). Exaples of the analysis of some planar reflectrors based on the photonic band gap technology were shown in [14] with a good agreement between the theory and the experiment. More specifically, antennas in [14] were analyzed by CST Microwave Studio, which is currently the only FIT solver available on the market.

Radiation properties of planar reflector antennas were also studied with respect to the available broadband beahaviour. Such a study is also given in the thesis, where the measured gain bandwith of the designed planar reflector antennas is compared.

---

[1] Finite-Difference Time-Domain method

1.2 AIMS OF THE DISSERATATION

The presented dissertation is aimed to the development of efficient design strategies for simple and folded reflector antennas. As mentioned in previous chapters, much of the work has already been done in the filed. However, following issues have not been discussed in the literature yet:

Tuning patch dimensions has not been described in the open literature;
Radiation pattern calculations were not published or were described unclearly [1];

-No attention was turned to the consideration about the phase-center position of the feeder and its influence on radiation properties of the planar reflector antennas;
-Design of simple reflector antennas with non-canonical and electrically small reflectors has not been performed yet;
-Insufficient attention was turned to the tolerance analysis of the antennas with respect to the patch dimensions and dielectric permittivity.

In spite of these facts, a thorough design procedure of planar reflector antennas has been developed. Matlab implementation of the local optimization method is described. Together with tuning issues, strategies of the design of all kinds of planar reflector antennas are detailed.

Attention is paid to the post-processing of the antenna analysis results. The post-processing uses originally derived surface equivalence theorem (Huygens principle, also known as Kirchoff's integral. Expressions for the far field solution of the Kirchoff's integral are well known and easy to find in different papers. However, its version for the near filed is hard to find in the present literuature.

A particular sub-chapter is also dedicated to the derivation of alternative Green's functions for frequency selective surface (FSS) with a superstrate. The derivation given represents an extension of the theory presented in [6].

A portion of the work also deals with full-wave verifications of the designed antennas. Several simulations are presented. Results given are also supported by models of the antennas or associated structures in ENSEMBLE and ANSYS. A part of simulations in ANSYS is also original since it brings the experience in building large complex three-dimensional (3D) models via APDL (ANSYS parametric design language).

2 DESIGN OF PLANAR REFLECTOR ANTENNAS

The previous chapter explained briefly the arrangement of basic planar reflector antennas. As mentioned, the frequency selective surface (FSS) is a key part of any planar reflector antenna. During the design of the planar antenna, a particular cell of the reflectarray is assumed to be locally under a plane wave illumination and the cell is a part of an inifinite FSS. Analysis of the refleclection properties of the FSS is perfomed by the spectral domain method of moments.

2.1 PLANE WAVE REFLECTION FROM THE INFINITE FSS

Let us assume the situation shown in Fig. 2.1. The coordinate system and the orientation of the incident wave is chosen in accordance with [5].
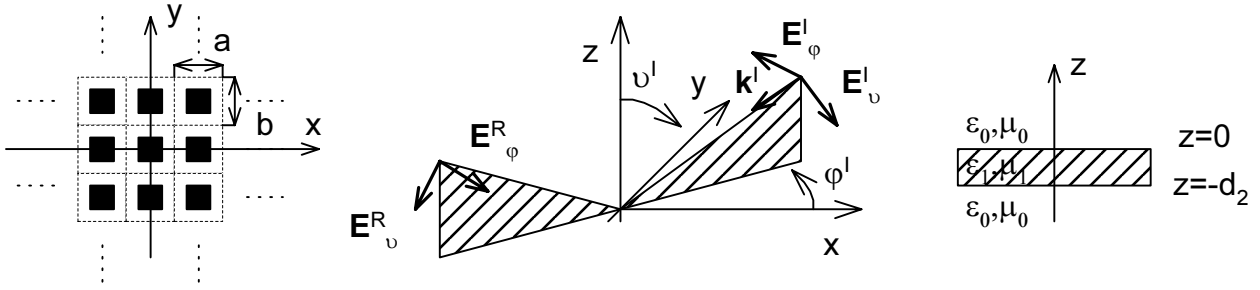

Fig. 2.1 *Infinite periodic array of identical patches (left), plane wave incidence on the FSS (right).*

Reflection from the FSS is described by the matrix of reflection coefficients [R]

$$[R]=\begin{bmatrix} \rho_{\vartheta\vartheta} & \rho_{\vartheta\varphi} \\ \rho_{\varphi\vartheta} & \rho_{\varphi\varphi} \end{bmatrix},$$ … (2.1)

where single reflection coefficients are defined as

$$\rho_{\vartheta\vartheta} = \frac{E_{\vartheta}^{R}}{E_{\vartheta}^{I}}; E_{\varphi}^{I} = 0 \dots$$ (2.2a) $$\rho_{\varphi\vartheta} = \frac{E_{\varphi}^{R}}{E_{\vartheta}^{I}}; E_{\varphi}^{I} = 0 , \dots$$ (2.2b)

$$\rho_{\vartheta\varphi} = \frac{E_{\vartheta}^{R}}{E_{\varphi}^{I}}; E_{\vartheta}^{I} = 0 \dots$$ (2.2c) $$\rho_{\varphi\varphi} = \frac{E_{\varphi}^{R}}{E_{\varphi}^{I}}; E_{\vartheta}^{I} = 0 , \dots$$ (2.2d)

Note!
Reflection coefficients defined in most papers doesn't use definition (2.2), but they relate directly z-transversal components of the electric field of incident and reflected waves. Since such definition is widely used in common literature (e.g. [3], [4]).

Determination of matrix [R] is based on a numerical solution of the electric field integral equation (EFIE) in the spectral domain. Its form for the FSS with two dielectric and one metal layer (assuming $e^{j\omega t}$ convence) is

$$\sum_{n=-N}^{N}\sum_{m=-M}^{M}[G_C][\mathbf{J}]e^{j(\alpha_m x+\beta_n y)} = -([I]+[R_{20}]\phi_2^2)[M_C]^{-1}2[K_{0mn}][X]\delta_{mn}\,\mathbf{E}_0^I e^{j(\alpha_0 x+\beta_0 y)}$$

$$\ldots \quad (2.3)$$

where corresponding Green's functions for the FSS are

$$[G_C]=([I]+[R_{20}]\phi_2^2)[M]^{-1}\frac{1}{2}([K_{1mn}][X](\phi_1+\phi_1^{-1})+[K_{0mn}][X](\phi_1^{-1}-\phi_1))([K_{1mn}][X])^{-1}[X]$$

$$[M_C]=[[K_{0mn}][X]([I]+[R_{20}]\phi_2^2)-[K_{1mn}][X]([I]+[R_{20}]\phi_2^2)+$$

$$\frac{1}{2}([K_{1mn}][X](\phi_1+\phi_1^{-1})+[K_{0mn}][X](\phi_1^{-1}-\phi_1))([K_{1mn}][X])^{-1}$$

$$([K_{2mn}][X]([I]-[R_{20}]\phi_2^2)+[K_{1mn}][X]([I]+[R_{20}]\phi_2^2))]$$

with $\phi_2=e^{-j\sqrt{k_2^2-\alpha_m^2-\beta_n^2}\,d_2}$ $\phi_1=e^{-j\sqrt{k_1^2-\alpha_m^2-\beta_n^2}\,d_1}$ being propagators in the substrate and superstrate (square root with negative imaginary part is taken), d_2 and d_1 [m] stand for thickness of the substrate and superstrate, [I] is a unit matrix and matix [X] is $[X]=\begin{bmatrix} 0 & 1 \\ -1 & 0 \end{bmatrix}$, structure of matrix $[K_{imn}]$ can be found in [6].

Application of the Galerkin procedure with suitable large domain current expansion functions ([5],[6]) results in a system of linear equations

$$\begin{bmatrix} U^{TETE} & U^{TETM} \\ U^{TMTE} & U^{TMTM} \end{bmatrix}\begin{bmatrix} C_{TE} \\ C_{TM} \end{bmatrix}=\begin{bmatrix} F_{TE} \\ F_{TM} \end{bmatrix}, \qquad \ldots \quad (2.4)$$

where the right hand side of the equation contains the known excitation field.

The system is solved for the unknown current expansion coefficients. With the aid of the coefficients, the current density and the total electric field on the most top dielectric layer of the FSS is obtained. Then, tangential components of the intensity of reflected wave are transformed into a spherical system and final reflection coefficients are obtained.

2.2 CONVERGENCE ISSUES REGADING PHASE OF REFLECTION COEFFICIENT

Accurate calculation of the phase of reflection coefficients for the reflectarray (FSS with patches on the grounded dielectric substrate) requires extremely precise modeling of patch currents. An example of convergence curve valid for the FSS shown in Fig. 2.2a is given in Graph 2.2b.
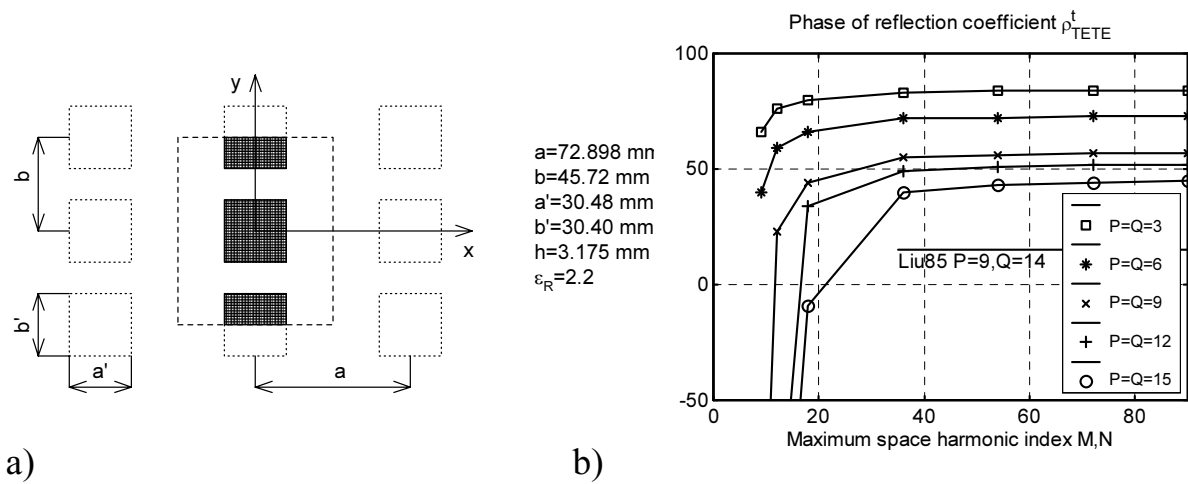
a)   b)

Fig. 2.2 *a) Microstrip patch array test case – dimensions. b) MoM convergence curves (solid lines, P, Q = 3 to 15 - trigonometric current expansion functions without edge singularity, Reference results (trigonometric basis with edge factors) [15] are shown by a straight line marked asLiu85.*

Even with the proper edge current modeling [15], a relatively high order of current expansion functions is needed for precise computation of the phase of reflection coefficients. Overall solution time is thus affected (matrix fill dominates the solution time because of high Floquet numbers M, N needed in double summations in eqn. 2.3). However, the total solution time and memory requirements are still adequate in comparison with the finite-element method (FEM) or FDTD which tend to comsume much more computational power to maintain the same degree of accuracy.

See for example the FSS from Fig. 2.2. The FSS was simulated by the waveguide simualor approach in Ansys 6 and FEM results were compared with MoM results for the same structure. Matlab code `fssrectg.m` (based on theory in book [6]) was used. In order to get a high accuracy of FEM results (phase error near resonance $<20\div30°$) very fine mesh around the central patch was necessary. See model details in Fig. 2.3.
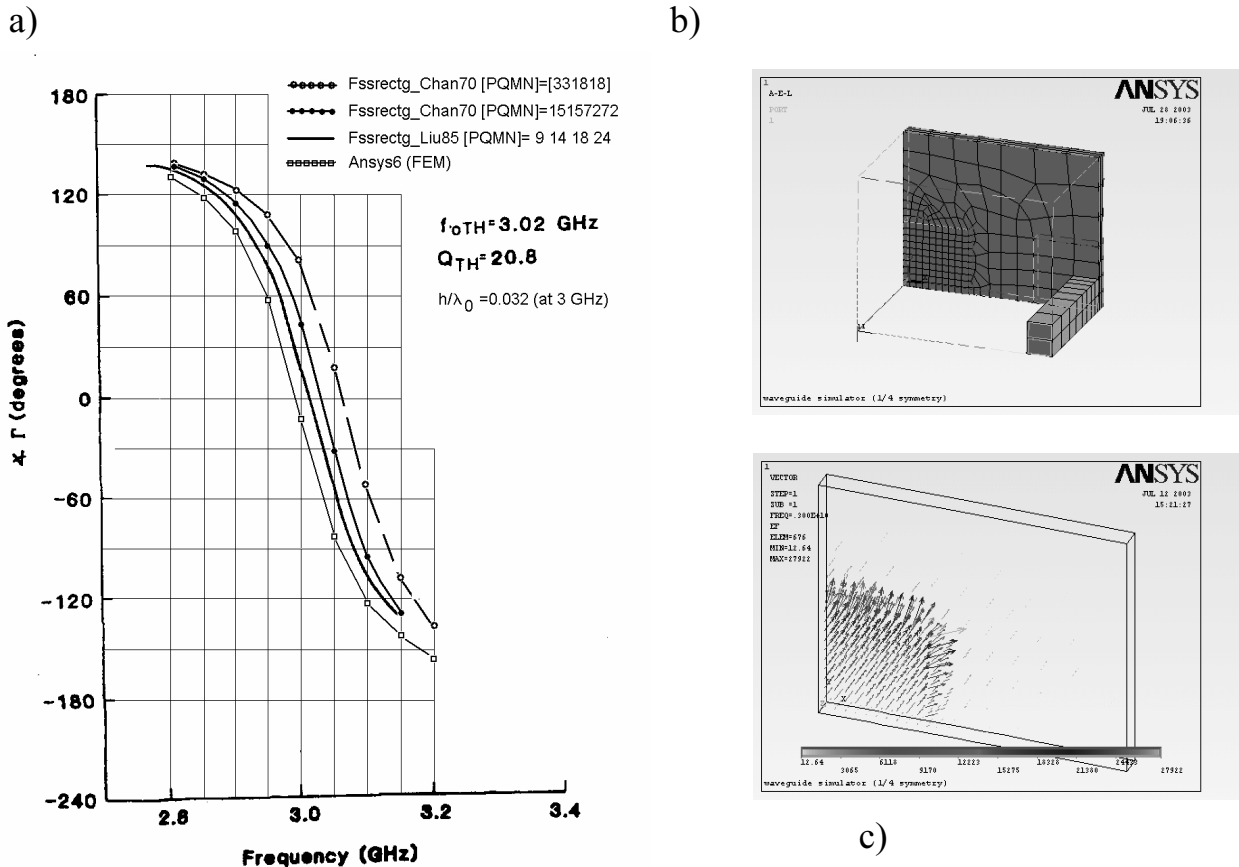
a)

b)

c)

Fig. 2.3 a) *Comparison of phase of reflection coefficient obtained by different approaches (details given in the text). b) Outline of the model of one quarter of the waveguide in Ansys6 used to simulate reflection from infinite array of patches. Because of clearity, only elements in the substrate volume together with few elements along z direction are shown. Total number of second order hexahedral elements is 53226. c) Vector plot of electric field at frequency 3 GHz*

2.3 USING LEVENBERG-MARQUARDT METHOD IN THE DESIGN OF PLANAR REFLECTOR ANTENNAS

The Levenberg –Marquardt method (LM) is a local optimization technique capable of minimization of a criterial function. The function can be represented by a vector multidimensional complex function. LV method is often referred as the quasi Newton's method. Let's assume a non-linear complex vector function $\mathbf{F}(\mathbf{x})$ as the object of the optimization. Further assume a vector $\mathbf{x}$ representing a vector of design variables (DV) x_j ($j=1..N$). Each component F_i ($i=1..M$) of the vector $\mathbf{F}$ is a non-linear complex function of variables $x_1..x_N$. Unknown DV's $x_1..x_N$ have to be found to satisfy the following relation

$$\left\| \mathbf{F}(\mathbf{x}) - \mathbf{F}_d \right\|^2 = \min \qquad \qquad \dots \quad (2.5)$$

where $\mathbf{F}_d$ ... is the vector of desired functional values

Initially, elements of the vector $\mathbf{x}$ (containing DV's) are initial values x_j, and such a vector is denoted as $\mathbf{x}_0$. Then, series of iterative steps is performed. At each lth iterative step ($l=1.. \ l_{max}$), the difference between functional values $\mathbf{F}(\mathbf{x}_l)$ and $\mathbf{F}_d$ is evaluated. The difference is then used to evaluate a "step increment" Δ_l. Series of iterative steps continue until the error norm (2.5) falls under a specified value or until the maximum allowed number of iterations is exceeded. The mathematical description of the iteration problem is as follows

$$([D]^H [D] + \alpha [I]) \Delta_l = [D]^H (\mathbf{F}_d - \mathbf{F}(\mathbf{x}_l)) \ , \qquad\qquad \text{...} \quad (2.6)$$

where $[D]$,   ... Jacobian of function $\mathbf{F}$ ($[D]_{ij} = \partial F_i / \partial x_j$)

           $[D]^H$ ... transposition and complex conjungate of Jacobian $[D]$

           α ... positive real number (regularization parameter)

           $[I]$ ... identity matrix of size $N \ x \ N$

           Δ_l ... step of vector $\mathbf{x}$ at l^{th} iteration (it holds $\mathbf{x}_{l+1} = \mathbf{x}_l + \Delta_l$)

To get the value of the vector Δ_l a direct inversion is performed:

$$\Delta_l = inv(([D]^H [D] + \alpha [I])) [D]^H (\mathbf{F}_d - \mathbf{F}(\mathbf{x}_l)) \qquad\qquad \text{...} \quad (2.7)$$

The value of parameter β is dependent on the difference $Err_l = \left\| \mathbf{F}_d - \mathbf{F}(\mathbf{x}_l) \right\|^p$ between the desired and an actual function value at current (l^{th}) and previous ($(l-1)^{th}$) iteration steps. If error decreases parameter remains the same. In case that the error varies only slightly, parameter β is reduced by one half. Such a reduction of β leads to an increase of the step length to get a faster convergence. Finally, last case that may happen is an increase of the error which must lead to a step length reduction by doubling parameter β.

```
LV method – application in design of reflectarrays
```

During the design of the reflectarray, the LV method is used to find patch dimensions which results in the desired phase of components E^R_x or E^R_y of the electric field of the reflected wave. Mathematically written, the following phase of the componets is required

$$\arg(E^R_x) = \mathrm{mod}(2\pi - \Delta\varphi, 2\pi) \ , \qquad\qquad\qquad \text{...} \ (2.8a)$$

$$\arg(-E^R_y) = \mathrm{mod}(2\pi - \Delta\varphi, 2\pi) \ . \qquad\qquad\qquad \text{...} \ (2.8b)$$

If a folded reflector antenna is considered, eq. (2.8b) is modified into

$$\arg(-E_y^R) = \mathrm{mod}(2\pi - \Delta\varphi - \pi, 2\pi) \ . \qquad\qquad\qquad \ldots (2.8\mathrm{c})$$

A typical dependence of phase of components E_x^R or E_y^R on patch dimensions is shown in Fig. 2.4. The dependance is not a monotonic function of patch dimensions. There is a step change of phase at resonance). To handle the step change correctly, a modification of the original LV method [16] is necessary. The modification is related to the case when error norm increases only slightly. In such a case, original application in [16] admitted further step change, which could in certain cases result in overcoming a local minimum. Such a possibility had to be disabled in order to prevent jumping from one side of the E_x^R (or E_y^R) surface plot to the other side. Except of that modification, incorporation of linear constraints on patch dimensions is introduced.

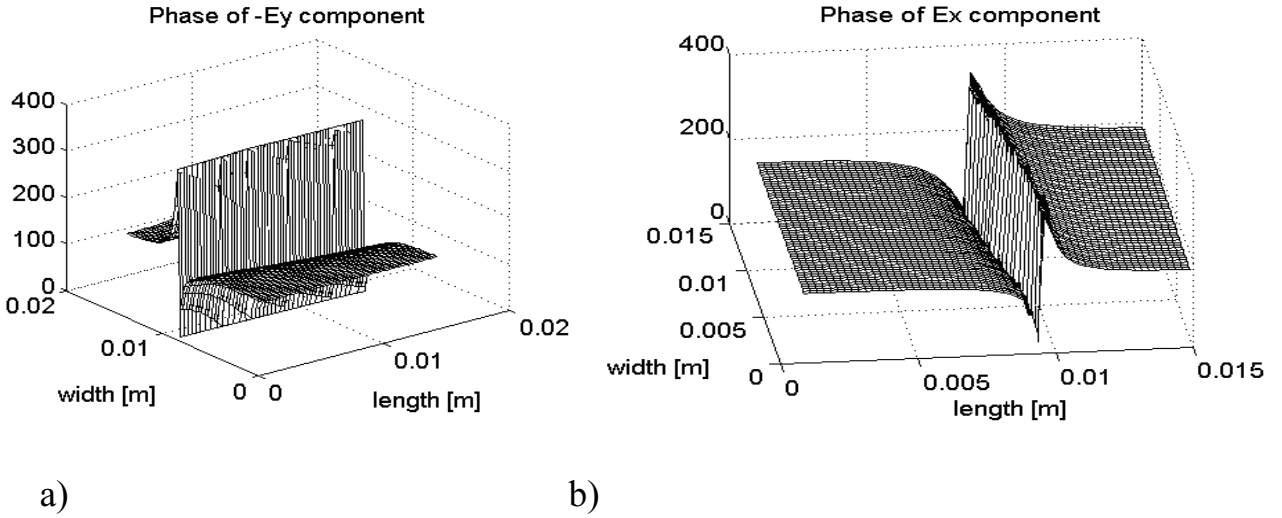
a)   b)

Fig. 2.4 *Phase of components of electric intensity of the reflected wave versus patch dimensions – a typical behaviour (substrate thickness 1.5 mm, relative permittivity 2.22, cell dimensions 16 x 16 mm, angle of incidence $\upsilon^I = 30°$ and $\varphi^I = 45°$ were assumed).*

An optimization is sucessful (design of patch dimensions) if the initial patch dimensions are set according to these equations

```
Simple reflector antenna
```

$$a'_{initial} = a'_{max}/3, \ b'_{initial} = b'_{max}/3 \ \text{ if } \ \Delta\varphi < 0.5(\varphi_1 + \varphi_2) \qquad \ldots (2.9\mathrm{a})$$
$$a'_{initial} = 3a'_{max}/4, \ b'_{initial} = 3b'_{max}/4 \ \text{ if } \ \Delta\varphi >= 0.5(\varphi_1 + \varphi_2) \qquad \ldots (2.9\mathrm{b})$$

```
Folded reflector antenna
```

14

$$a'_{initial} = a'_{\max}/3, \ b'_{initial} = 2b'_{\max}/3 \ \text{if} \ \Delta\varphi < 0.5(\varphi_1 + \varphi_2) \qquad \dots \quad (2.10a)$$

$$a'_{initial} = 2a'_{\max}/3, \ b'_{initial} = b'_{\max}/3 \ \text{if} \ \Delta\varphi >= 0.5(\varphi_1 + \varphi_2) \qquad \dots \quad (2.10b)$$

Here, values φ_1 and φ_2 define the region $<\varphi_1, \varphi_2>$ which cannot be achieved. The value of φ_1 is between 120 and 160 degrees (depending on the electrical thickness of the substrate) while the value of φ_2 is slightly less than 180 degrees.

2.4 REFLECTARRAYS – DESIGN STEPS

Design of the reflectarray (planar reflector antenna) consists of three major steps

I.   Preprocessing (choice of antenna topology, appropriate feeder, overall dimensions and material properties)
II. Tuning of patch dimensions (performed by an optimization technique)
III. Postprocessing (radiation pattern calculation, geometry exports)

These steps (as implemented in Matlab in the program `Rarray`) are going to be described here in more detail.

I.   Preprocessing

The step represents a selection of an appropriate antenna topology (simple or folded), main reflector diameter D, its thickness h, and permittivity ε_R. The reflector diameter D is determined according to the requirements on directivity and expected aperture efficiency of the antenna (typically 50% for a simple reflector antenna and 70% for a folded one). The physical thickness h of the main reflector is chosen according to the operating frequency. A typical value of the electrical thickness of the substrate is ~0.05λ.

The auxiliary reflector (or a slot array) has to be designed and placed at an appropriate height L above the main reflector. The height L has a meaning of an electrical or a physical height depending on the type of the designed antenna (simple or folded). For a folded antenna, the height L represents a physical height of the slotarray above the main reflector. The height is selected to fulfill –10dB edge taper on the main reflector. For a simple reflector antenna, the distance L represents a height of the phase center of a sub-reflector above the main reflector. In such a case, -10dB edge tapper on the edge of sub-reflector has to be fulfilled too. The situation for both versions (simple and folded) is shown in Fig. 2.5. A selection of radius of the sub-reflector is done iteratively in several steps to fulfill –10dB edge tapers on both the main reflector and sub-reflector edges. Incident field on the sub-reflector has to also approximately represent a plane wave because the assumption about the plane wave illumination was made during the phase center extraction of

the sub-reflector. The topic is briefly mentioned in chapter 2.6. Typically, the 20°
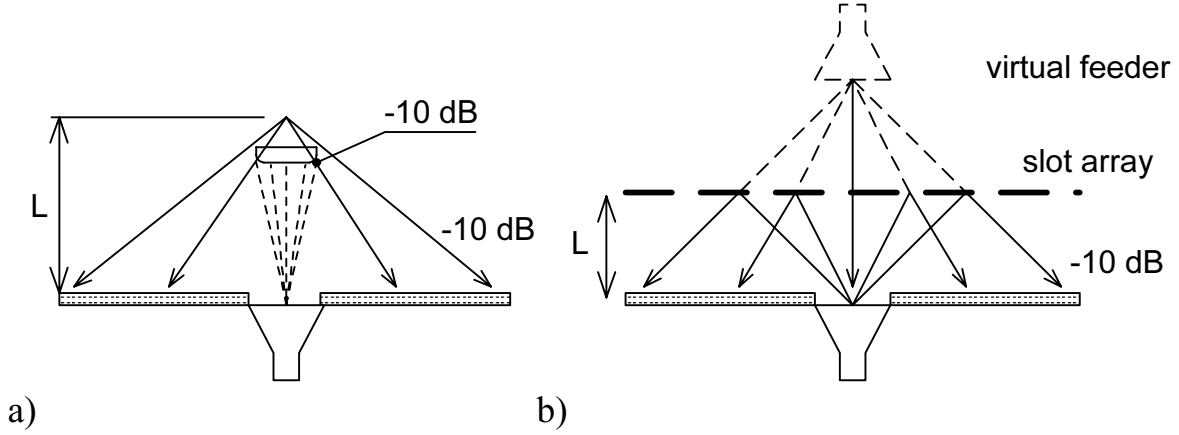phase change on sub-reflector edges with respect to its center is admitted.

Fig. 2.5 *Selection of main (sub-reflector) diameters according to edge taper (a)
simple reflector antenna (b) folded reflector antenna*

As the last part of preprocessing, cell dimensions (~ 0.5λ) and MoM solver
parameters *P,Q,M,N* are selected. Parameters *P,Q,M,N* depend on the type of current
basis functions being used. Typical values of P,Q for SIN()COS() basis with no edge
singularities are from six to twelve depending on the electrical thickness of the
substrate.

II. Tuning of patch dimensions

Tuning can be described as follows

1. A circular or rectangular layout of cells is generated. This is done according to
   the main reflector diameter *D* and the cell size *a*.
2. The program `Rarray` then goes through all cells of the reflector (if no symmetry
   is assumed) and evaluates phase delay for a particular cell with respect to the
   central cell. Then, either function `setshift_sngl.m` or
   `setshift_fold.m` is called. The function first determines the interval of
   unattainable phases $<\varphi_1,\varphi_2>$ is determined. In the next step, initial patch
   dimensions [*a', b'*] are selected according to eq. (2.9) or (2.10). After executing
   the function `Levmark.m`, final patch dimensions are returned. Each call of the
   function `Levmark` takes usually 3 to 5 iterations if the required phase of
   $[E^R_x,-E^R_y]$ components lies in the steep area of the phase versus dimensions curve
   (with a default value of the phase square error set to 2°). More iterations are
   necessary if the required phase approaches to φ_1 or φ_2. If the phase in the range
   $<\varphi_1,\varphi_2>$ is required, the maximum number of iterations (15 by default) is
   performed and the function `Levmark` returns patch dimensions with maximal or
   minimal dimensions because of constraints activation. The phase error is then

greater, typically about 10 to 20 degrees (depending on the electrical thickness of the substrate of the main reflector).

3. As the last step, program `Rarray` considers reflectarray symmetry.

III. Postprocessing

During the postprocessing in Matlab, the far-field radiation patterns are calculated. The procedure is the same for a simple and folded reflector antenna and it relies on a direct summation of contributions of the reflected electric field from individual cells to get the total value of the electric intensity of field radiated by the antenna.

$$
\mathbf{E}_\vartheta^f = \sum_{nc=1}^{Nc}\left[-\frac{jk}{4\pi}Z_0\int_{cel\,\ln nc}\mathbf{J}_{eq}^{nc}(x,y)\bullet\mathbf{T}_{xyz\_\vartheta}\frac{e^{-jk(r+\Delta_{nc})}}{r}dS\right]+\left[-\frac{jk}{4\pi}\int_{cel\,\ln nc}\mathbf{K}_{eq}^{nc}(x,y)\bullet\mathbf{T}_{xyz\_\varphi}\frac{e^{-jk(r+\Delta_{nc})}}{r}dS\right]
$$

$$
\mathbf{E}_\varphi^f = \sum_{nc=1}^{Nc}\left[-\frac{jk}{4\pi}Z_0\int_{cel\,\ln nc}\mathbf{J}_{eq}^{nc}(x,y)\bullet\mathbf{T}_{xyz\_\varphi}\frac{e^{-jk(r+\Delta_{nc})}}{r}dS\right]+\left[-\frac{jk}{4\pi}\int_{cel\,\ln nc}-\mathbf{K}_{eq}^{nc}(x,y)\bullet\mathbf{T}_{xyz\_\vartheta}\frac{e^{-jk(r+\Delta_{nc})}}{r}dS\right]
$$

…(2.11a,b)

where vectors T_{xyz_ϑ} and T_{xyz_φ} perform transformatiom from Cartesian to spherical system, $\mathbf{J}_{eq}^{nc}$ and $\mathbf{K}_{eq}^{nc}$ are densities of equivalent electric and magnetic current densities in a particular cell, k is free-space wavenumber and finally stands for free-space impedance Z_0. Evalution of integrals in (2.11) with the assumption on illumination of a particular cell by a plane wave results in the expression

$$
\begin{bmatrix}E_\vartheta^f\\E_\varphi^f\end{bmatrix}=\sum_{nc}-\frac{jk}{4\pi}\begin{bmatrix}Z_0\mathbf{J}_{eq}^{nc}\bullet\mathbf{T}_{xyz\_\vartheta} & \mathbf{K}_{eq}^{nc}\bullet\mathbf{T}_{xyz\_\varphi}\\Z_0\mathbf{J}_{eq}^{nc}\bullet\mathbf{T}_{xyz\_\varphi} & -\mathbf{K}_{eq}^{nc}\bullet\mathbf{T}_{xyz\_\vartheta}\end{bmatrix}C\frac{e^{-jkr}}{r}\qquad\dots\quad(2.12)
$$

with $C=ab\sin c(\frac{1}{2}k_xa)\sin c(\frac{1}{2}k_yb)$, $k_x=-\alpha_0+k\sin\vartheta\cos\varphi$, $k_y=-\beta_0+k\sin\vartheta\sin\varphi$

where $\alpha_0=k_0\sin(\vartheta^I)\cos(\varphi^I)$; $\beta_0=k_0\sin(\vartheta^I)\sin(\varphi^I)$ are negative projections of the wave vector of the incident plane wave in the center of a cell. Angles ϑ, φ are angles definining observation direction in a spherical system.

2.5 PLANAR REFLECTOR ANTENNAS – EXAMPLES

2.5.1 Simple reflector antenna at X band

As an example of a simple reflector antenna, an antenna operating at 10 GHz and having diameter $D = 200$ mm is given. The antenna uses the non-hyperbolic sub-reflector depicted in Fig. 2.5a. The height of the phase center of the sub-reflector

17

above the main reflector considered during the design of the main reflector was $L = 89$ mm. Substrate of the reflector had thickness 1.575 mm and permittivity 2.22). The antenna design assumed MoM solver parameters P,Q,M,N = 6,6,54,54 and took ~ 7 hours. Due to the symmetry, only half of the array was tuned, other half was copied appropriately. The layout of the main reflector and far-field radiation patterns of the reflectarray are shown in Fig. 2.6a, and Fig. 2.8a, b.
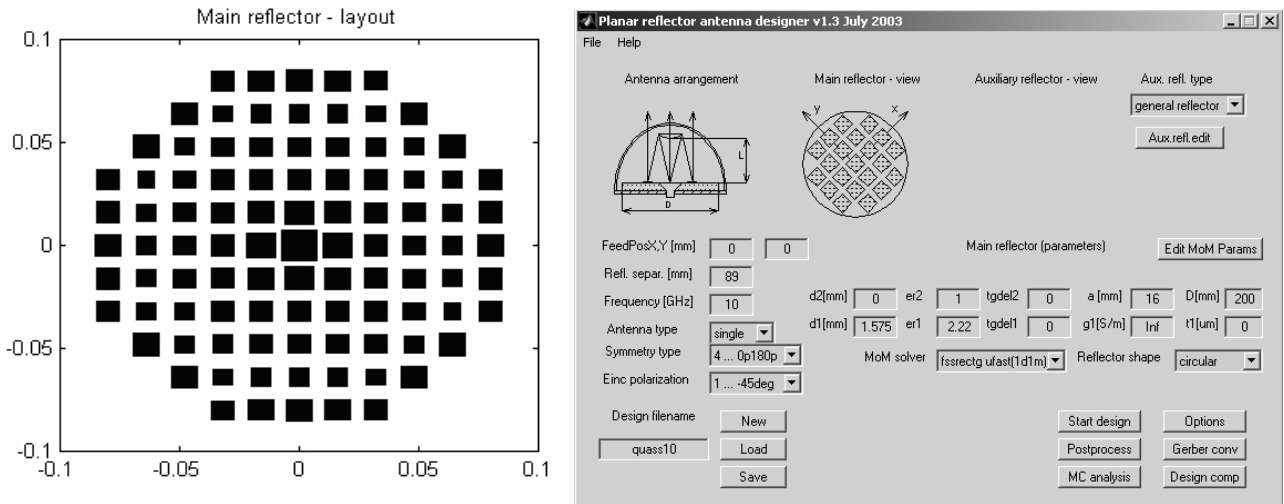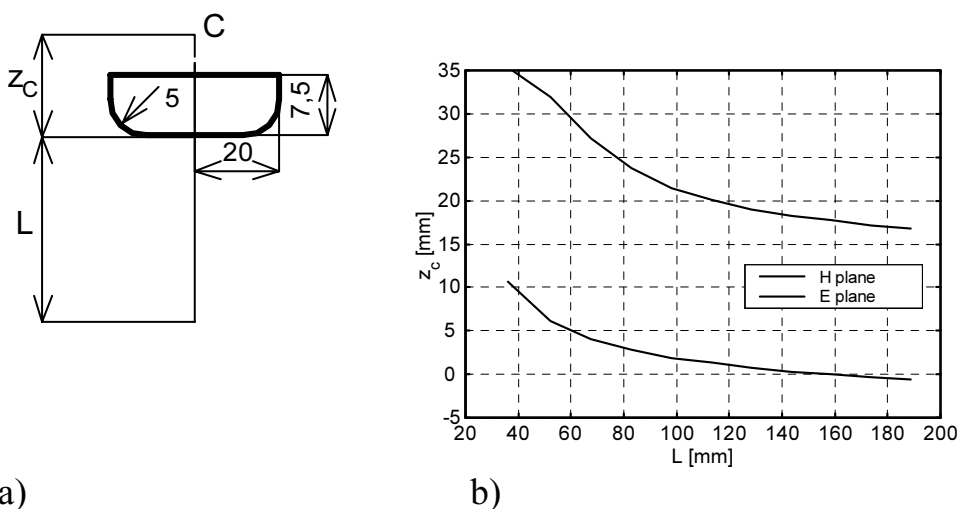

a)   b)

Fig. 2.6   *a) Layout of the main reflector of a simple reflector antenna at 10 GHz (dimensions in meters). b) Program Rarray - main screen.*

In order to verify behaviour of the complete antenna, fullwave simulations in Ansys and Lc (FDTD code from Cray research) were performed. Solid and finite element model in Ansys is shown in Fig. 2.9.

a)   b)

Fig. 2.7   *a) Subreflector – dimensions b) extracted phase center position of the reflector for E and H plane (Ansys6) as a function of observation distance*
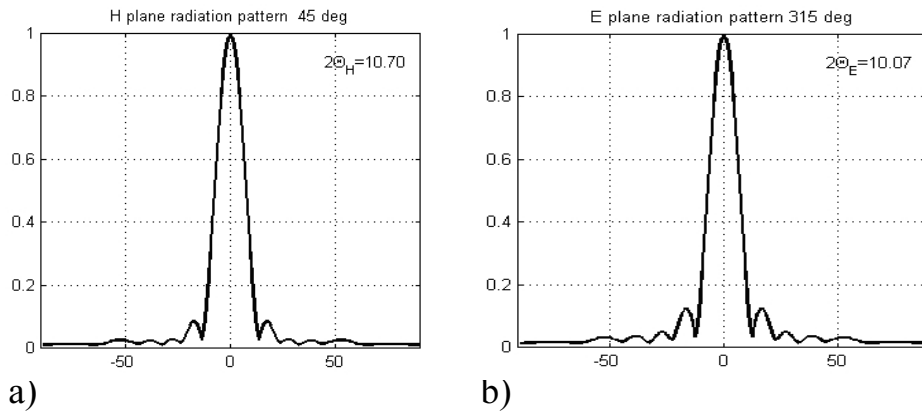
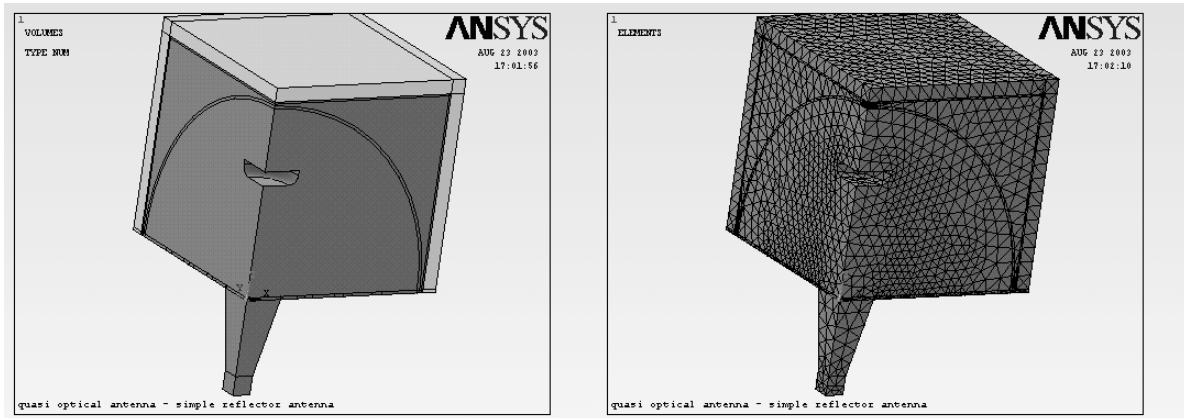**Fig. 2.8**   *Simulated radiation patterns – Matlab a) E plane b) H plane*

Fig. 2.9   *Solid (left) and finite element model the X-band simple reflector antenna in Ansys (61982, 2nd order tetrahedral elements, 379676 unknowns).*
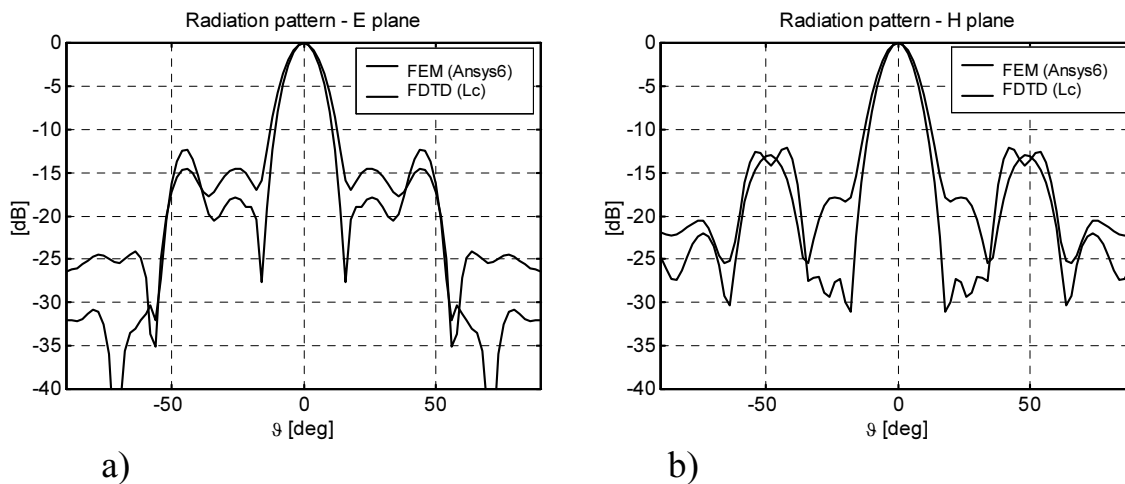

Fig. 2.10   *Comparison of simulated radiation patterns in Ansys (FEM) and Lc (FDTD).*

The simple reflector antenna operating in X band showed simulated gain about 20 dB (Both `Ansys` and `Lc`). Maximum directivity was D = 26.4dBi. Thus D/D_{max} ratio is about 23% Simulated sidelobe level is between 12 to 15 dB. Gain bandwidth for 1 dB loss is approximately 2.5 %.

2.5.2 Folded reflector antenna at K band

As an example of the folded reflector antenna, the same antenna as in [2] was designed and built in order to make comparison. The antenna operates at the frequency 20 GHz and has the diameter D = 130 mm of the main reflector. Substrate of the main reflector is Isoclad 917 (thickness 1.575 mm, permitivitty 2.22 (at 10 GHz)). An auxilialiry slot array is placed at the distance of L = 50 mm. The slot array is made from the same material and its cell has dimensions 9×4 mm with 6.8×1 slots. Cell and slot dimensions were designed by Matlab program `fssrectg2.m` which is an aperture version of `fssrectg.m` code. The antenna design assumed MoM solver parameters P=Q=3, M=N=18. Even when using current basis function with no edge singularities, the order of expansion functions P,Q could be small (because of the electrically thick (h/λ_0) substrate of the main reflector).

a)   b)

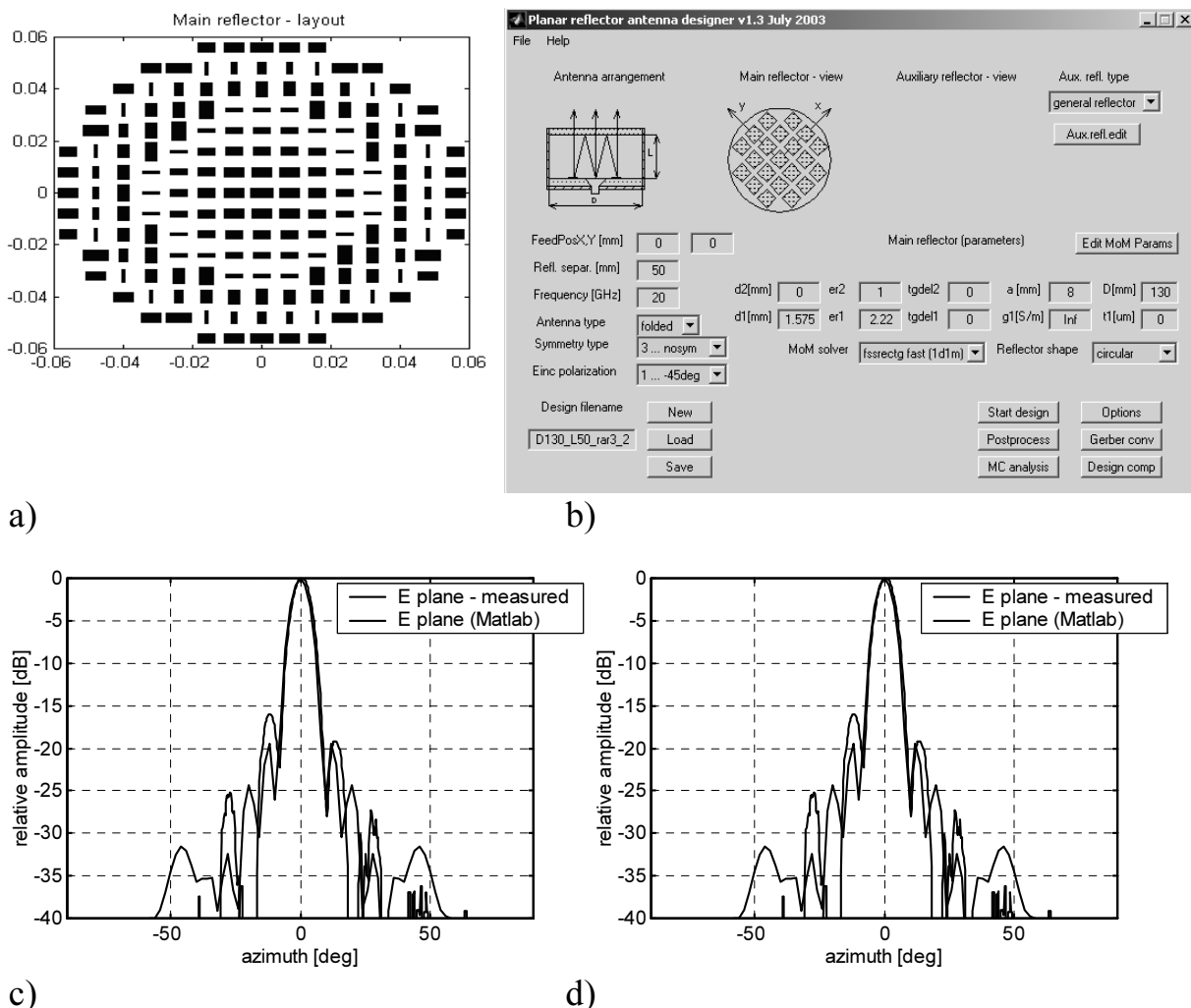c)   d)

Fig. 2.11 *a) Layout of the main reflector of the folded reflector antenna at 20 GHz (dimensions in meters), b) Program Rarray main screen c) d) E(H)-plane far-field radiation patterns in Matlab versus measured patterns (elevation angle in degrees)*

The layout of the main reflector and far-field radiation patterns of the antenna designed in Matlab are shown in Fig. 2.11a, c, d.

The folded antenna is being fed by a circular horn with aperture diameter $D_a = 20mm$. The horn is attached to the waveguide via a coaxial transition. The complete folded antenna was measured within an anechoic chamber. Measured gain of the antenna was about ~23 dBi at 20 GHz with 3 GHz gain bandwidth (1dB gain loss assumed) (Fig.2.12a). Sidelobe level at the central frequency was 16dB in E plane and 15 dB in H plane. All frequencies within 1 dB gain bandwidth showed side lobe level at least 15 dB or better (Fig. 2.12b).

The complete folded antenna was also simulated by FDTD. Fullwave analysis of the folded antenna was computationally very CPU-power demanding (because of the lack of symmetry).
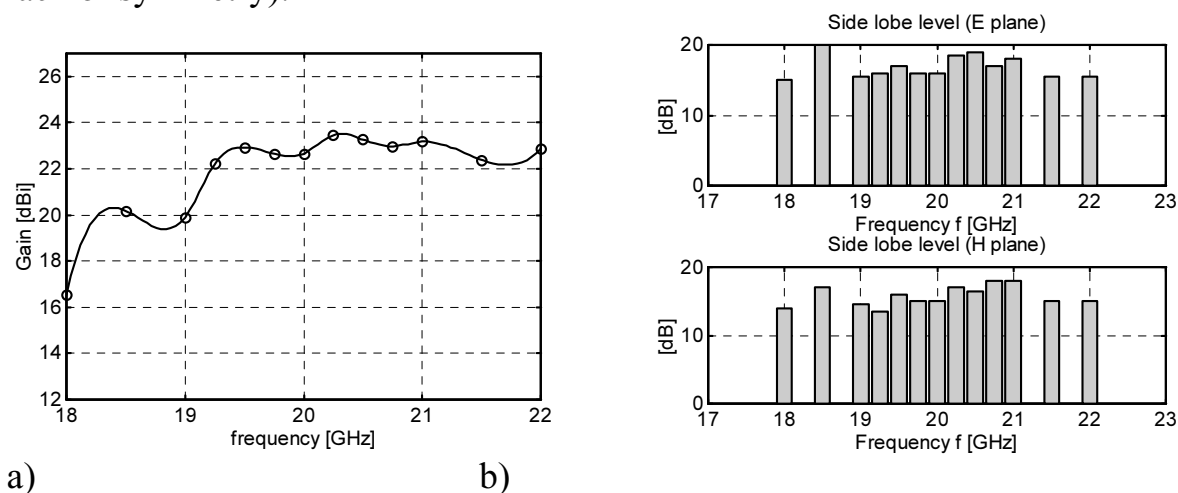

a)   b)

Fig. 2.12 *a) Measured gain of the folded antenna b) Measured side-lobe level on discrete frequencies*

A complete simulation took approximately 72 hours (Atholon 1.2 GHz, 768MB Ram, Win2000) and needed more than 1 GB of memory to finish marching through all time steps. Despite of the long run time, meaningful results were obtained by the simulation (at least the angular prediction of first two side lobes shows a good correlation with experiment, Fig. 2.13). Side lobe level prediction is relatively poor but it could be further improved by finer meshing. However, such a refined model would have to be simulated on a small cluster and not on a single PC.
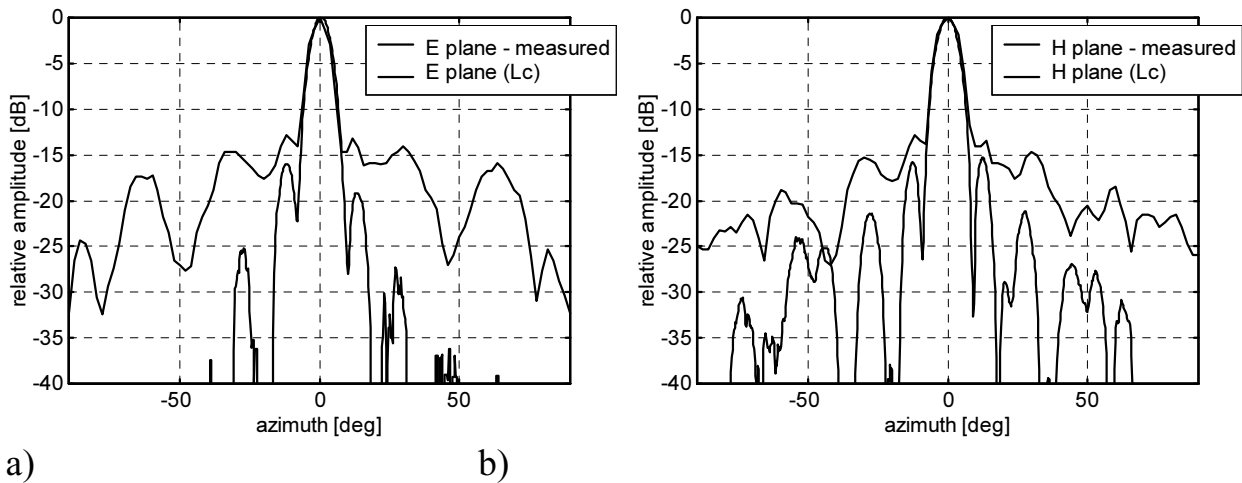
Fig. 2.13 *Measured and computed (FDTD) far field radiation patterns.*

2.5.3   Folded reflector antenna at Ka band

The operating frequency of the antenna was f = 34 GHz. Diameter of the main reflector and height of the antenna were D = 120 mm and L = 30 mm. As a substrate of the main reflector, 0.508 mm thick Diclad870 (ε_R=2.33 at 10 GHz and ε_R=2.50 in Ka band) was used. Cell period of the reflectarray was a = 4.5 mm. Slot array of the folded antenna was fabricated from an substrate FR4 having (ε_R = 4.7 at *Ka* band). Cell and slot dimensions were again designed by the program `fssrectg2.m`. Resulting cell and slot dimensions were 4×3.2 and 3×1 mm.
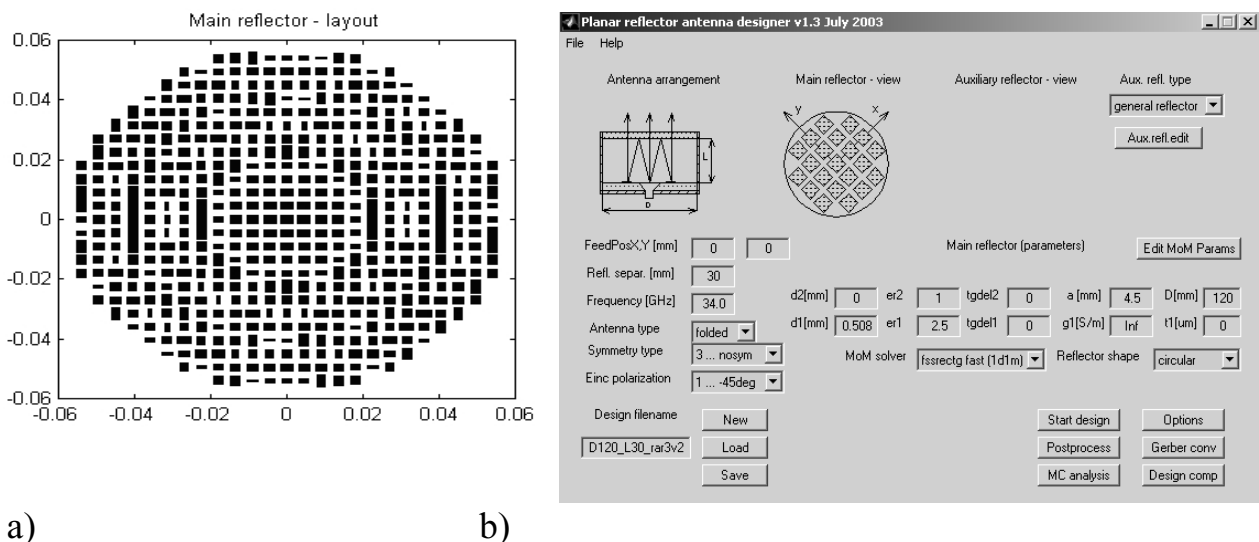

Fig. 2.14 *a) Layout of the main reflector of folded reflector antenna at 34 GHz (dimensions in meters), b) Program* `Rarray`*- main screen*

The antenna design assumed MoM solver parameters P=Q=3, M=N=18. Since the main substrate is relatively thick (~$0.058\lambda_0$), higher values of P,Q,M,N are needed to reach convergence. Study of convergence of phase of reflection coefficient showed that values P=Q=9, M=N=54 are adequate (phase of reflection coefficient with error ±5°). Such high values were not used for the design of the reflectarray for two reasons. First, at the time when the layout of the folded antenna for 34 GHz was generated (May 2002), convergence issues about code `fssrectg.m` were not clarified completely. Second, even if the converge issues were known that time it would be impossible to run design because of long solution time of `fssrectg` for high values P,Q. Total design time of the reflectarray (with 505 patches) for P=Q=3, M=N=18 and using code `fssrectgf` was 8 hours and 40 minutes (Atholon 1.2 GHz). Design of the same reflectarray but considering P=Q=9, M=N=54 and `fssrectgu` (a faster version of code `fssrectgf`) as the FSS core solver takes 63 hours.

The layout of the main reflector of the *Ka* band reflectarray as designed by program `Rarray` considering P=Q=3, M=N=18 and code `fssrectg` as the core MoM solver are shown in Fig. 2.14. The simulated E and H plane beamwidth of the designed reflectarray is $\Theta_E = 4.8°$ and $\Theta_H = 4.6°$. Thus the gain of the antenna as predicted from the radiation patterns is G=27000/($\Theta_E\Theta_H$)=27000/(4.8·4.6)=30.9 dBi. Real gain of the folded antenna will be smaller because of phase errors in the reflectarray, mismatch and dielectric loss. A maximum directivity for the antenna having a diameter of 120 mm is $D_{max} = 32.8$dBi. The predicted sidelobe level is approximately 20 dB in both planes.

The folded antenna is being fed by a circular horn having a half power beamwidth $\Theta_E = 24°$ and $\Theta_H = 20°$. The subtended half angle of the folded antenna is about $\vartheta_0 = 45°$. Radiation pattern of the horn can be approximated as a $\cos^4(\vartheta)$, which together with the angle ϑ_0 gives resulting aperture efficiency η_a=73%.

The designed folded antenna was built and measured. E plane radiation patterns and the gain of the antenna are shown in next figure. Measured gain was about 28.3 dBi which is less than expected from radiation patterns (30.9 dBi). The difference is influenced by phase errors in the reflectarray, mismatch loss and also due to a relatively small seperartion between main reflector and the slotarray. Gain bandwidth of the antenna was approximately 2.5 GHz (2 dB gain loss).
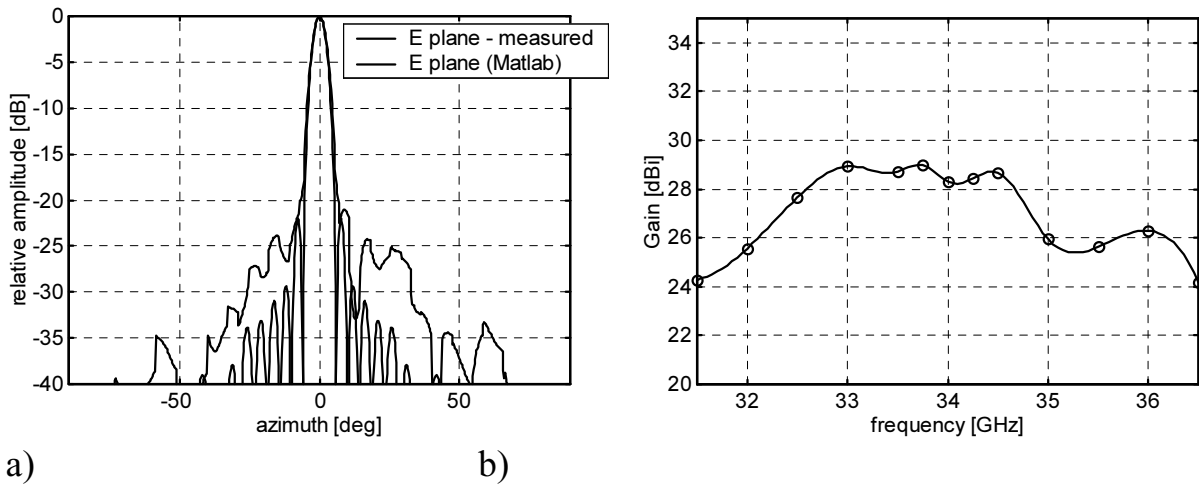
Fig. 2.15 *a) measured radiation pattern (E plane) at 34 GHz   b) measured gain*

It is expected that the gain of the antenna can approach to gain of a traditional parabolic antenna if appropriate design steps are taken. But even now, measured results looks quite good (G = 28dBi) in comparison with the parabolic antenna (G = 30dBi) having the same diameter.

2.6   PHASE CENTER EXTRACTION OF ANTENNAS AND SCATTERERS

A procedure of numerical extraction of the phase center of an antenna or a scatterer was developed. The method relies on a full-wave EM simulation of the antenna (or a scatterer). After performing the EM simulation outgoing wavefronts for different observation distances are constructed are phase center position is determined from simple geometric relations. One example of the extracted phase center position was given in Chapter 2.5., where the depenence of the phase center of the non-hyperbolic subreflector on an observation distance was given.

Another example related to the phase centers is shown in next figure (Fig. 2.16) where behaviour of the phase center of a horn antenna is studied. It can be seen that phase center position for a given observation distance is different in E and H planes. Asymptotic behaviour of the curves in Fig. 2.16 is that E and H phase centers appear in the ground plane level for the infinite observation location.

A complete description of issues related to the exctration of phase center of antennas and scatterers can be found found in Jina2002 conference paper ([10]).
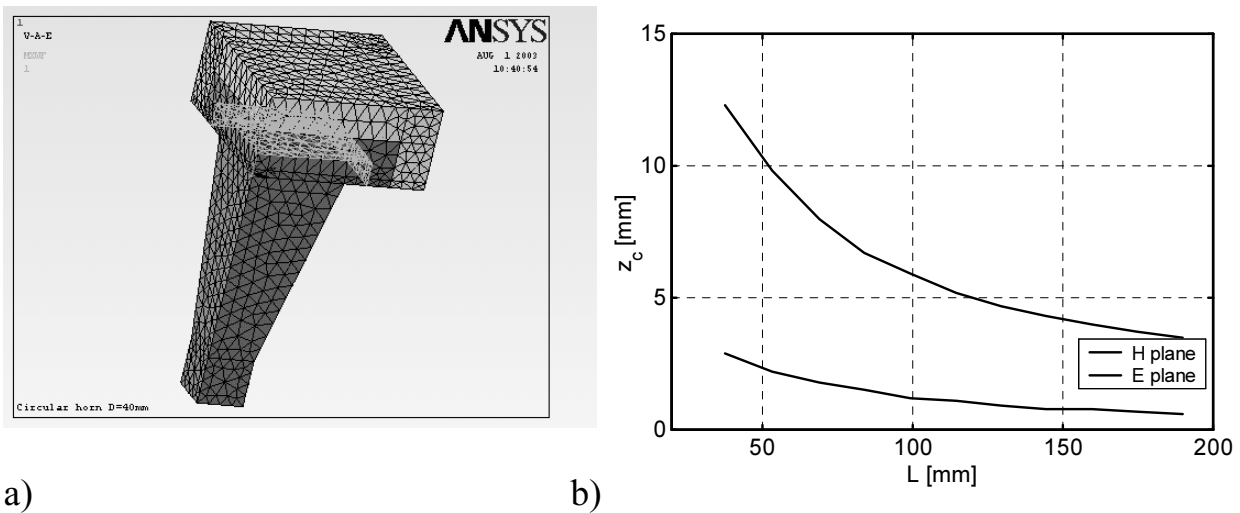
Fig. 2.16   *a) Solid and finite element model of circular horn antenna within infinite ground plane in Ansys6. Antenna is fed by circular waveguide (diameter 20 mm, TE$_{11}$ mode, electric field is y-polarized). Total number of first order HF119 tetrahedral elements is 60346. Solution time at single frequency f = 10 GHz is about 8 mins (Celeron 433 MHz, 288MB). b) Phase center position z$_c$ below ground plane as a function of observation distance L above ground plane.*

2.7   ANALYSIS OF PRINTED STRUCTURES BY SPATIAL DOMAIN MOM

A part of the dissertation was also dedicated to the development of the simulator `Rebeca`. The code can be used for anlysis of small printed structes by the spatial method of moments. The simulator was primarily used for verification of the spectral domain code `fssrectg.m`. More specifically a comparitive study about current distribution on a single patch of the infite FSS was performed. Such a study helped to prove correctness of code `fssrectg.m` and in conjuction with other approaches (like waveguide simulator in `Ansys`) helped to the make conclusions about the convergence of the MoM solutions (both in space and spectral domain).

The characteristics of the simulator are as follows:

- analysis of printed structures with a single metal and dielectric layer
- collocation technique
- possible use of non-equidistant mesh but with a limit on mesh non-uniformity
- limitation on maximum axial ratio of charge and current cells is set to 5
- different excitation mechanisms (port fed (vertical, horizontal delta gap voltage sources) or plane wave illuminated). Combination of port and plane wave is also possible

- approximate Green's functions for modeling of substrate effects (ε_R and $h/\lambda <= 0.05$)
- restriction on single port circuits.
- Several de-embedding mechanisms (localized, wave, horizontal stub)
- Basic visualization capabilities for current and input impedance.
- Text/command line input of the geometry of printed structure.

a)

b)

c)

d)

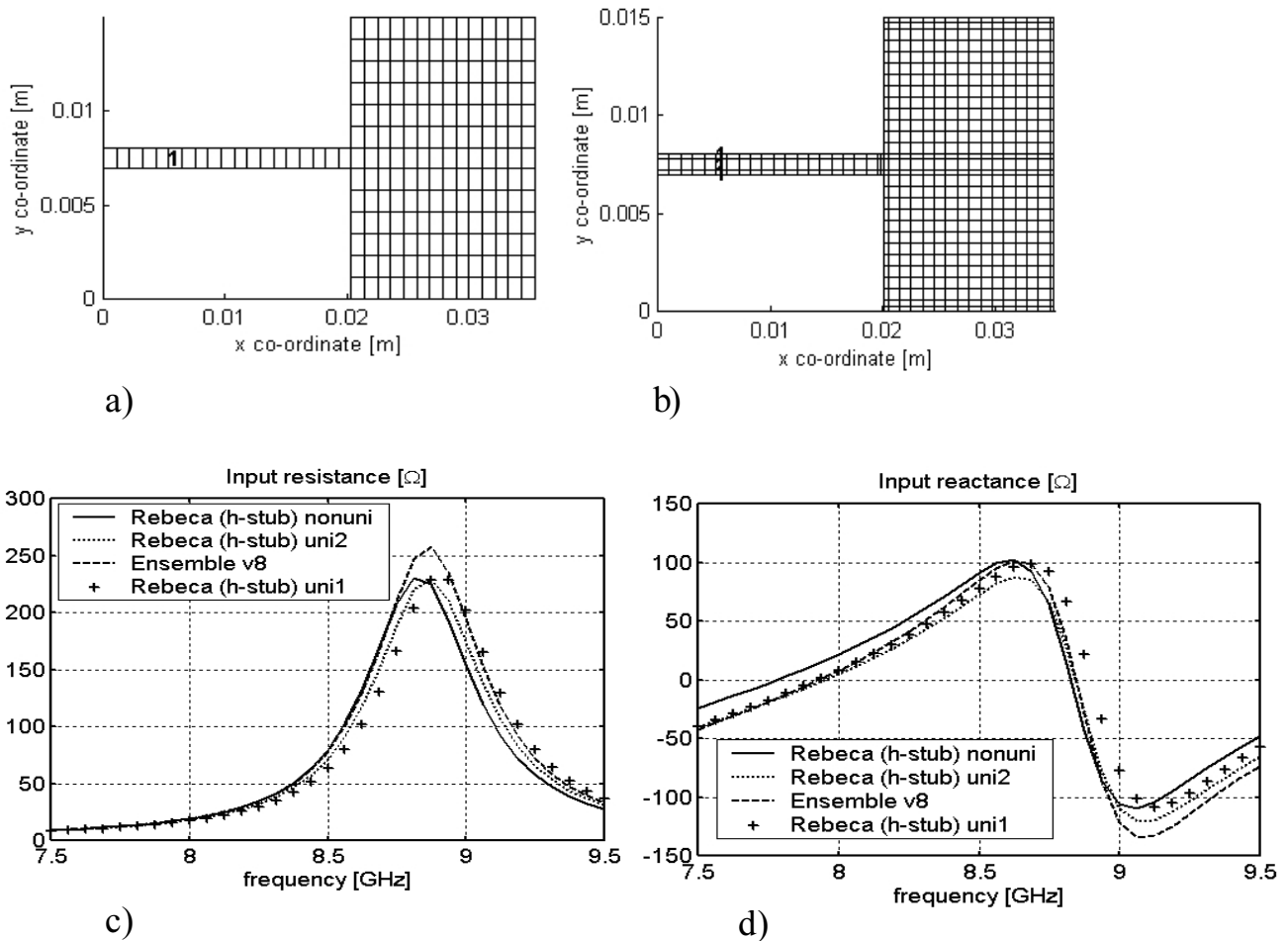**Fig. 2.17** *a) uniformly meshed patch b) patch with thin edge cells c) (d) input resistance (reactance) of rectangular patch as computed in Rebeca simulator using edge port with horizontal stub de-embedding. Abbreviations uni1 and uni2 mean uniform mesh with coarse (uni1) and fine (uni2) mesh density. Results obtained from non-uniformly meshed patch model are shown in solid line (abbr. Nonuni).*

3   CONCLUSIONS

The dissertation demonstrated strategy for design of planar reflector antennas. The approach used relied on the numerical analysis of reflection from from printed reflectarrays by the spectral domain method of moments in conjunction with a fast local optimization method. A big attention was dedicated to the accuracy of computation of phase of reflection coefficient from the infinite frequency selective surfaces (FSS). A comparison of convergence of the phase of reflection coefficient for different methods (namely MoM and FEM) was presented. Numerical analysis of the FSS by the method of moments also resulted in original derivation of Green's functions for the FSS with two dielectric layers. The functions derived are of different form than the same functions obtained by the well-known immitance approach developed by T.Itoh. Of course, both functions are equivalent which means that they produce the same results when analyzing reflection/transmission from the two layred FSS. A necessity for computation of complete radiation pattern of the planar reflector antennas led to a need for a self-derivation of surface equivalence principle. Such a derivation was done prior to the same results (also known as Kirchoff's integral) were found in appropriate papers.

On the basis of the design procedures proposed for the planar reflector antennas, three planar reflector antennas were designed. All antennas were verified carefully. Either the fullwave simulations or experiments were used to verify correctness of the `Rarray` program, which was written in `Matlab` to support design of planar reflector antennas. The agreement between theoretically predicted characteristics of planar antennas and measured results was found relatively good. The complete version of the dissertation also discusses impact of etch errors and dielectric permitivity variation on gain reduction of planar reflector antennas. It also presents a comparative study about broad-band behaviour of the planar reflector antennas available in the present literature and antennas designed in this thesis.

Except of the program `Rarray`, a separate simulator `Rebeca` was developed as a product of the thesis. That simulator is also deeply described in the thesis. A big focus is put on the realization fast analytical evaluation of all integrals arising in the spatial domain MoM. Partial attention is paid to feeding of printed structures. Associated de-embeddig issues were discussed too.

4 BIBLIOGRAPHY

[1] POZAR, D. M., TARGONSKI, S. D., SYRIGOS, H. D. Design of Millimeter Wave Microstrip Reflectarrays. *IEEE Proceedings on Antennas and Propagation.* Feb. 1997, vol. 45, pp. 287-295.

[2] PILZ , D. , MENZEL, W. Folded Reflectarray Antenna. *Electronic letters.* April 1998, vol. 34, pp. 832 - 833.

[3] PILZ, D. , MENZEL, W., LEBERER, R. A 77-GHz FM/CW Radar Front-End with a Low-Profile Low-Loss Printed Antenna. *IEEE Proceedings on Microwave Theory and Techniques.* Dec. 1999, vol. 47, pp. 2237–2241.

[4] ENCINAR, J. A. Design of Two-Layer Printed Reflectarrays Using Patches of Variable size. *IEEE Trans. Microwave theory and technique.* Oct. 2001, vol. 49, pp. 1403 – 1410.

[5] MITTRA, R. , CWICK, T. , CHEN, C. H. Techniques for Analyzing Frequency Selective Surfaces – A Review. *IEEE Proceedings.* Dec. 1988, vol. 76, pp. 1593 – 1615.

[6] SCOTT, G. Spectral Domain method in electromagnetics. *Artech House,* 1900, *London.*

[7] GOŇA, S. Computer design of frequency selective surfaces. *diploma thesis* (*in Czech*). 1999, Brno.

[8] JAVOR, R. D. , WU, X. D., CHANG, K. Design and performance of a microstrip reflectarray antenna. *IEEE Trans. Antennas and propagation.* Sept. 1995, vol. 43, pp. 932 – 938.

[9] CHANG, D. , C., HUANG, M. C. Multiple Polarization Microstrip Reflectarray Antenna with High Efficiency and Low Cross Polarization. *IEEE Trans. Antennas and propagation.* Aug. 1995, vol. 43, pp. 829 – 834.

[10] PILZ. D., MENZEL, W. Periodic and quasi-periodic structures for antenna applications. *Proceedings of the conference COMITE 1999.* pp. 311 - 314.

[11] MENZEL. W., TIKRIRITI, M. Al. , LEBERER, R. A 76 GHz Multiple-Beam Planar reflector Antenna. *Proceedings of the European Microwave Conference.*, Milano 2002.

[12] PILZ, D. , MENZEL, W. Mixed integration method for the evaluation of the reaction integrals using the spectral domain method. *IEE Proceedings on Microwave Antennas and propagation.* June 1999, vol. 146, pp. 214 - 218.

[13] FERESIDIS, A. P., VARDAXOGLOU, J.C. *International conference on electromagnetics in advanced applications* (Iceaa 2001). Sept. 10-14, 2001, Torino, pp. 243-246.

[14] MENZEL, W. , AL-TIKRITI, M. Low profile, narrow-beam antenna with a printed periodic structure. International symposium on antennas (JINA 2002), Nice 12-14 Nov 2002, vol. 2, pp.97-100.

[15] LIU, C. C. , HESSEL, A. , HANFLING, J.D., USOFF, J.M. Plane wave reflection from microstrip patch arrays – Theory and Experiment. *IEEE Trans. Antennas and propagation.* Apr. 1985, vol. 33, pp. 426 – 435.

[16] FRANCHOIS, A. , PICHOT, C. Microwave imaging – complex permittivity reconstruction with Levenberg-Marquardt method. *IEEE Trans. Antennas and propagation.* Feb. 1997, vol. 45, pp. 203 – 215.

5 SELECTED PUBLICATIONS OF THE AUTHOR

[1] GOŇA, S., RAIDA, Z. Hybrid FE/SD MoM analysis of frequency selective surfaces with arbitrarily shaped elements. *International conference on electromagnetics in advanced applications (ICEAA99).* Sept. 13-17, 1999. Torino – Italy.

[2] GOŇA, S. Levenberg Marquardt method and its application in microwave technique. *Proceedings of student's jobs (in Czech).* June 2000, vol. 2, pp. 319-320, Brno – Czech Republic.

[3] GOŇA, S., RAIDA, Z. A planar reflector antenna for FMCW automotive Doppler radar. *International conference Radioelektronika 2000.* Sept. 12-13 , 2000, Bratislava – Slovakia.

[4] GOŇA, S., RAIDA, Z. Computationally efficient analysis of planar structures by method of moments. *International conference Radioelektronika 2001.*, May. 10-11 , 2001, Brno – Czech Republic, pp. 242-245, ISBN 80-214-1861-3.

[5] GOŇA, S., RAIDA, Z. Computationally efficient analysis of planar structures by method of moments. *International conference on electromagnetics in advanced applications (ICEAA01).* Sept. 10-14 , 2001, Torino – Italy, pp. 481-484.

[6] GOŇA, S., RAIDA, Z. Matlab based MoM simulator. *In proceedings of conference COMITE 2001.* Sept. 2001, pp. 73-76, Pardubice – Czech Republic, ISBN-8090241794.

[7] RAIDA, Z., ČERNOHORSKÝ, D. ,GALA, D.,GOŇA, S.,MICHÁLEK, V.,NAVRÁTIL, V.,NOVÁČEK, Z.,OTEVŘEL, V.,POMĚNKA, P.,ŠEBESTA, J.,URBANEC, T.
A multimedia textbook of EM theory and techniques. In proceedings of the 16th International conference on Applied Electromagnetics and Communications ICECOM 2001. ICECom 2001. Dubrovník (Croatia). KoREMA, 2001, pp. 216-220, ISBN 95-360-3736-X.

[8] GOŇA, S. , RAIDA, Z. A study of influence of dielectric cover on FSS properties ". *Proceedings of international conference Radioelektronika 2002.*, vol. XX, pp. xxx - xxx, May 2002.

[9] GOŇA, S. , RAIDA, Z. Design of planar reflector antennas. *Radioengineering.*, vol. 11, No 3., pp. 7 - 13, Sept. 2002.

[10] GOŇA, S. , RAIDA, Z. Phase center extraction of antennas and scatterers. *International symposium on antennas JINA 2002.*, vol. 2, pp. 249 - 252, Nov. 12-14, 2002.

BIOGRAPHY

Date of birth: 19.8.1976
Place of birth: Slavičín
Nationality: Czech
Education

1990-1994   Technical Secondary School Zlín
1994-1999   Brno University of Technology (BUT),
                   Faculty of Electrical Engineering and Computer Science
1999-2002   BUT, Faculty of Electrical Engineering and Communication
                   Internal doctoral studies at the Dept. of Radio Electronics

Praxis

Oct2000-Jan2001   Katholique Hogeschool Brugge-Oostende, Belgium
                   Analog CMOS design

2002-present   Ramet c.h.m., a.s. , Kunovice
                   Research engineer (microwave circuits and antennas)

Language knowledge:

English   FCE, June 2000

Reserach activities:

Numerical analysis by the method of moments, finite element analysis in Ansys,
near field technology, antenna design and measurements, design of passive and
active microwave circuits.

ABSTRAKT

Dizertační práce se zabývá problematikou analýzy a návrhu planárních reflektorových antén. První část práce popisuje současný stav vývoje v této oblasti. Jsou přitom zmíněny podstatné odkazy na literaturu, ve které byla diskutována numerická analýza těchto antén. Druhá část práce diskutuje úlohu pasivních planárních odražečů, jejich analýzu a vztah ke kmitočtově selektivním povrchům (modelovaných pomocí spektrální momentové metody). Syntéza (návrh) takovýchto struktur probíhá za pomocí rychlé lokální optimalizační metody (Levenberg-Marqurdt). Pozornost je věnována také ověřovaní vlastností navržených reflektorových antén, a to jak experimentálně tak i numericky (za pomocí *fullwave* elektromagnetické analýzy).

Práce se soustřeďuje na několik hlavních problémů. Prvním z nich je přesnost výpočtu fáze činitele odrazu od kmitočtově selektivních povrchů. Jsou přitom srovnávány výsledky momentové metody a výsledky získané metodou konečných prvků s ohledem na konvergenční vlastnosti a výpočetní náročnost. Je také diskutována otázka výběru vhodných bázových funkcí použitých k modelování proudového rozložení na periodických selektivních površích s obdélníkovými elementy.

Druhou, velmi významnou částí práce je implementace lokální optimalizační techniky pro účely dolaďování fáze jednotlivých elementů planární reflektorové antény. Kromě vlastní implementace je věnována pozornost vhodnému výběru počátních podmínek optimalizace (rozměrů fázovačů) s ohledem na rychlost a úspěšnost optimalizace. Dále je v práci demonstrována náhrada klasických pomocných hyprerbolických subpreflektorů za subreflektor jiného, výrobně jednoduššího tvaru. Za tímto účelem se provádí numerický výpočet fázového středu takovéto reflektoru. Použita je přitom metoda konečných prvků v Ansysu. Konečně poslední částí dizertace je popis vývoje *fullwave* simulátoru určeného k analýze planárních struktur momentovou metodou v prostorové oblasti. Tento simulátor je použit k ověřování chování kmitočtově selektivních povrchů, a to na základě srovnání s výsledky získanými spektrální momentovou metodou.

Práce obsahuje několik originálních odvození týkajících se kmitočtově selektivních povrchů, výrazů pro blízkozónní podobu Kirchoffova integrálu, ale také Greenových funkcí v uzavřeném tvaru platných pro planární struktury.